Analysis of Bow Shapes Proposed on a High-Speed Displacement Hull

Franklin J. Domínguez Ruiz[1,2(✉)], Lino Andrés García Jaramillo[1], and Patrick Roger Townsend Valencia[3]

[1] TECNAVIN S.A., Guayaquil, Ecuador
jdominguez@tecnavin.com, lagarcia@espol.edu.ec
[2] Universidade da Coruña - UDC, A Coruña, Spain
[3] ESPOL, Guayaquil, Ecuador
ptownsen@espol.edu.ec

Abstract. This study uses the computer fluid dynamic (CFD) software to compare the resistance between six different bow shapes for a high-speed displacement hull – type NPL. To begin, the original forms of a conventional shape hull are compared between the resistance results from tank test measurements with the CFD results. Then, six bow shapes are also proposed and analyzed, including a bulbous bow, wave piercing bow, axe bow, modified axe bow, and reverse piercing bow; these shapes are sized according to analytical and experimental recommendations. At final on this research, a new hull bow shape is proposed: by adding a ballast bulb to the axe bow to improve ship performance. The CFD resistance calculation is performed for calm water, while for the sea condition is considered added resistance estimation, calculated from seakeeping analysis. A predictive resistance analysis has been performed to show ship behavior and compared with the CFD results. Finally, the seaworthiness analyses of the models are calculated using strip theory to compare the ship comfort and performance of the six studied models.

Keywords: CFD · High speed ship · Bow · Optimization

1 Introduction

Reducing ship CO2 emissions, fuel consumption, and operating costs have gained importance over the last few decades. Currently, hull form optimization is a significant factor in improving ship performance and seaworthiness, and has been studied extensively for example: Takahei (1960) and Takahei (1961) introduced a bulbous bow in the hull to realize a wave less hull form. Keuning et al. (2002) performed towing tank test for the axe bow concept founding improving to the seakeeping behavior and operability compared to a conventional bow hull. In this paper a conventional hull form has been studied using a tank test with a model of the ship, obtaining model results including resistance and propulsion tests that can be transferred to a full-scale hull according to ITTC recommendations.

V. A. J. E. Carreño Moreno et al. (Eds.): CIDIN 2019/COPINAVAL 2019, pp. 89–103, 2020.
https://doi.org/10.1007/978-3-030-35963-8_8

Computer fluid dynamics (CFD) is the numerical modeling of fluids that allows the interactions of liquids, gases, and solids. Initially, tank test results of a conventional bow hull are compared with the CFD software results for validation. The expected results for this study will allow a determination of which of the studied bow shapes shows the best performance with regard to hull resistance, dynamic pressure, and free surface elevation as well as heave and pitch for six different models.

2 Analysis of Hull Bow Shapes

The study compare bow shapes developed in previous studies that where tested independently, as Wigley (1936), Hirota et al. (2005) and Keuning et al. (2002). Five different bow shapes shown in Figs. 2, 3, 4, 5 and 6 are proposed for a comparison with conventional hull

Model 1. The first model is a conventional high-speed displacement hull, type NPL. It measures 45 m in length and has an optimized hull form in basin tests. The conventional hull shape is shown in Fig. 1 and its characteristics are given in Table 1.

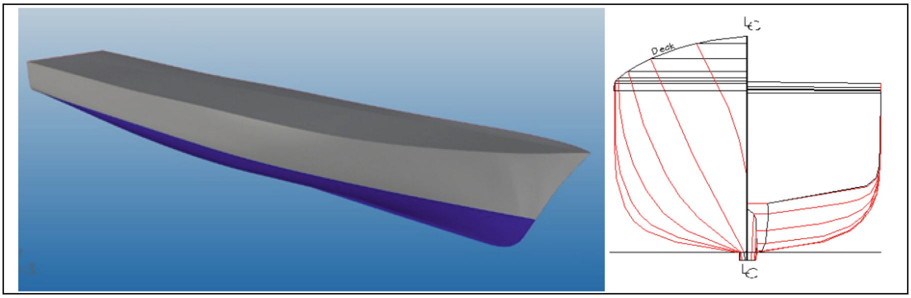

Fig. 1. Conventional optimized hull shape – Model 1

Table 1. Model 1, principal dimensions

Main characteristics		
Overall length	45.0	m
Beam	7.0	m
Depth	4.0	m
Draft	1.85	m

Model 2. The second model is the same as Model 1, with the addition of a bulbous bow of the Nabla type (see Kyriazis 1996). The bulb lies below the waterline and protrudes by 1 m. The Model 2 hull shape is shown in Fig. 2.

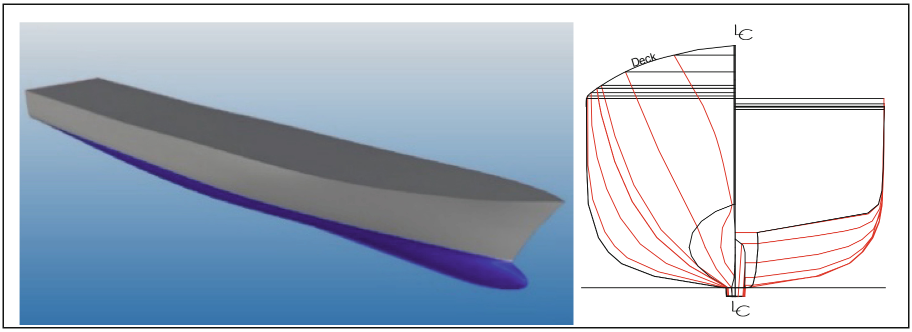

Fig. 2. Bulbous bow – Model 2

Model 3. The third model follows the dimensions of Model 1 and adds a wave piercing bow as well as a new fine body form just above the waterline. Its body protrudes 2 m from its original shape. The Model 3 hull shape is shown in Fig. 3.

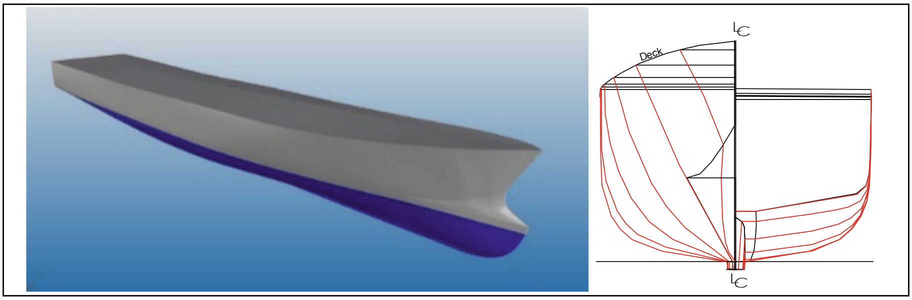

Fig. 3. Added wave piercing – Model 3

Model 4. The fourth model, the axe bow, has a completely vertical wave piercing bow, which increases the ship's overall length by 6 m; it also has a very fine bow shape without flare. The Model 4 hull shape is shown in Fig. 4.

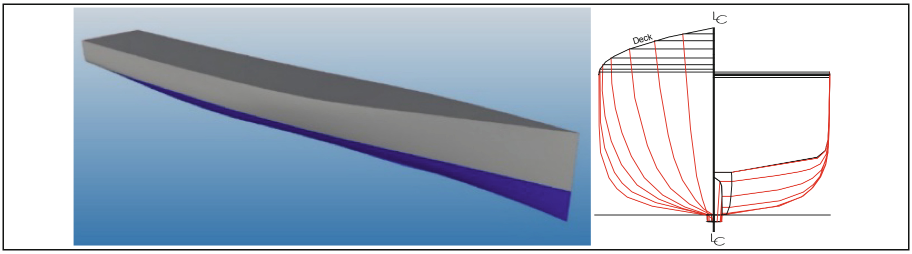

Fig. 4. Axe bow – Model 4

Model 5. The fifth model has a modified axe bow. This means that the hull body below the waterline is modified from Model 4, and a ballast bulb is added. The Model 5 hull shape is shown in Fig. 5.

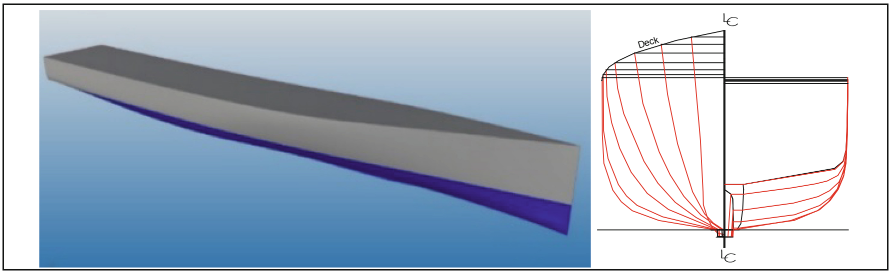

Fig. 5. Modified axe bow – Model 5

Model 6. The final model has an inverted bow. This increases the ship's length below the waterline, obtaining a finer bow, a bow flare, and a bulb at the lower forward point. The ship's overall length is increased by 3 m. The Model 6 hull shape is shown in Fig. 6.

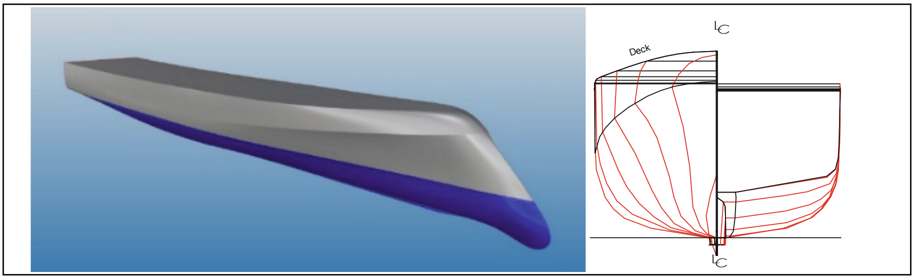

Fig. 6. Inverted bow – Model 6

3 Tank Test Results

A tank test experiment was carried out on Model 1. The results for the ship bare hull resistance in calm water are presented in Table 2.

Table 2. Tank test results for conventionally shaped - Model 1

Ship speed	Resistance	Froude	Heave	Pitch
[kn]	[kN]	Fnv	[m]	[°]
14	41.6	0.8919	−0.12	−0.11
16	65.6	1.0193	−0.17	0.04
17	84.2	1.083	−0.2	0.27
18	104.2	1.1467	−0.22	0.54
19	124.1	1.2104	−0.23	0.84

4 CFD Test Condition

The six ship models detailed in Sect. 2 were tested under the same load conditions and without considering weight increase or center of gravity modification. The results are shown in Table 3.

Table 3. CFD test conditions

Speed	19	Kt
Displacement	294	Ton
Hull rugosity	0.15	Mm
Initial trim	0	Degrees
Sea state	–	Calm water

5 CFD Results (Calm Water)

Each model's results for resistance, heave and pitch performance were obtained from the CFD software and are shown in Table 4. The results are compared with the conventional hull shape in Table 5.

Table 4. CFD results at 19 knots

Model	Resistance	Heave	Pitch
	N	M	degrees
1. Conventional	124486	−0.210	−0.943
2. Bulbous bow	119986	−0.216	−0.864
3. Wave piercing	112310	−0.210	−0.845
4. Axe-standard	82286	−0.172	−0.478
5. Axe-bulb	80606	−0.172	−0.449
6. Inverted bow	96324	−0.209	−0.506

Table 5. CFD results compared to the conventional Model 1

Model	Resistance	Heave	Pitch
	Reduction	Difference	
2. Bulbous bow	4%	−3.1%	8.4%
3. Wave piercing	10%	−0.2%	10.3%
4. Axe-standard	34%	17.9%	49.3%
5. Axe-bulb	35%	18.0%	52.3%
6. Inverted bow	23%	0.6%	46.3%

5.1 Free Surface Results (Calm Water)

Free surface is the contact surface between water and air. Free surface results demonstrate the waves generated by the ship in calm water. The free surface elevations in the wave patterns generated by the respective models are shown in Fig. 7; blue shows wave depression while magenta shows wave crest.

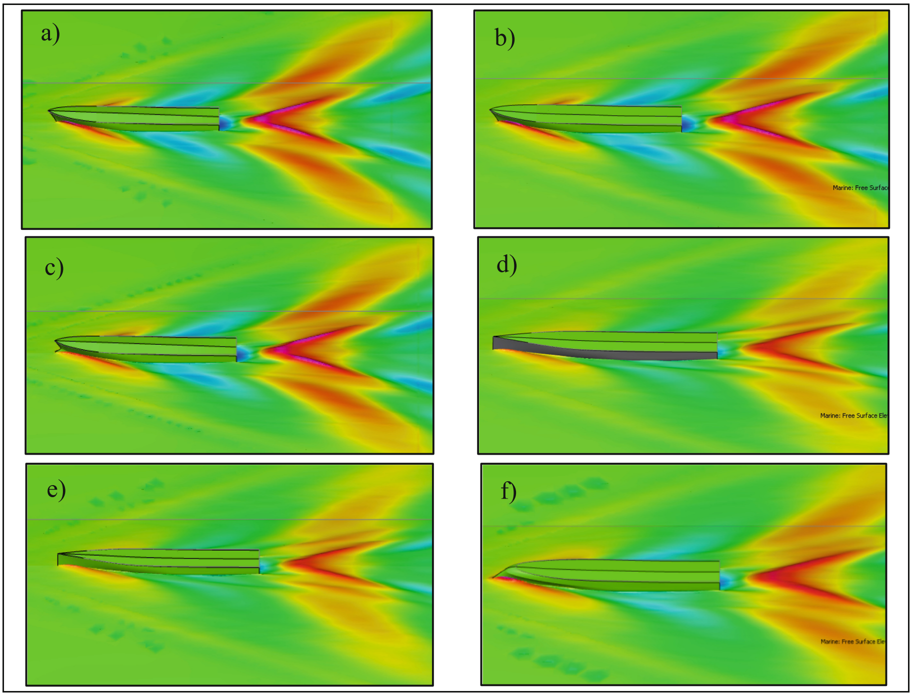

Fig. 7. Free surface elevation: (a) model 1, (b) model 2, (c) model 3, (d) model 4, (e) model 5, and (f) model 6

5.2 Bottom Dynamic Pressure Results

Bottom dynamic pressure is the pressure generated by the water due to ship movement. The results of the bottom dynamic pressures are shown in Fig. 8: (a) model 1, (b) model 2, (c) model 3, (d) model 4, (e) model 5 and (f) model 6.

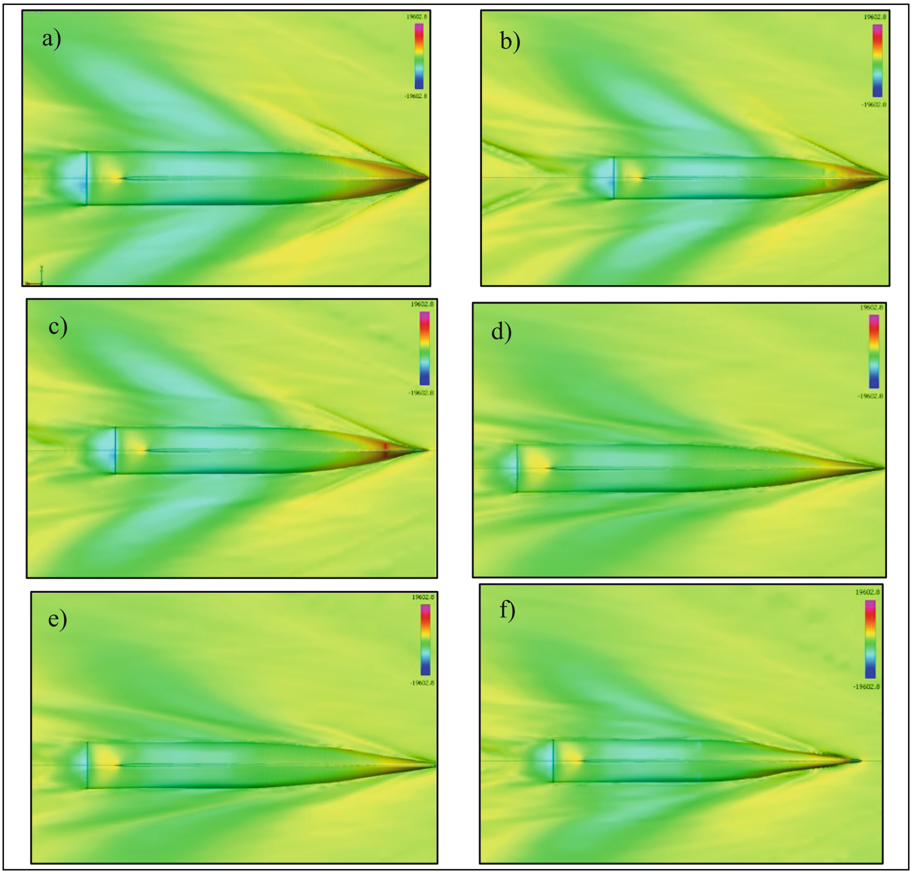

Fig. 8. Bottom dynamic pressure: (a) model 1, (b) model 2, (c) model 3, (d) model 4, (e) model 5, and (f) model 6.

6 Bare Hull Resistance Prediction Results

The preliminary resistance prediction analysis was determined with the Maxsurf Resistance software using two different methods, namely: Holtrop regression method (Holtrop 1984) and the Slender body method at different speeds in calm water. The tank test was performed only for the conventional hull, Model 1, thus, a regression resistance calculation was performed to provide a comparison with the CFD results.

Figure 9 and Table 7 show the resistance prediction using the Holtrop method (Holtrop 1982, 1984), which is based on the test results for certain types of ships.

The resistance calculated with the Holtrop method includes:

1. Frictional resistance according to the ITTC formulation – R_F
2. Form factor of the hull – $1 + k_1$
3. Appendage resistance – R_{APP}
4. Wave resistance – R_W
5. Additional pressure resistance due to a bulbous bow – R_B
6. Additional pressure resistance due to transom immersion – R_{TR}
7. Model-ship correlation resistance – R_A

The proposed ship hull characteristics meet the Holtrop method's requirements; see Table 6.

Table 6. Holtrop method's requirements

Parameter	Minimum value	Maximum value
Prismatic coefficient - CP	0.55	0.85
Waterline length/waterline breadth	3.90	14.90
Waterline breadth/draft	2.10	4.00
Froude number	0.10	0.80

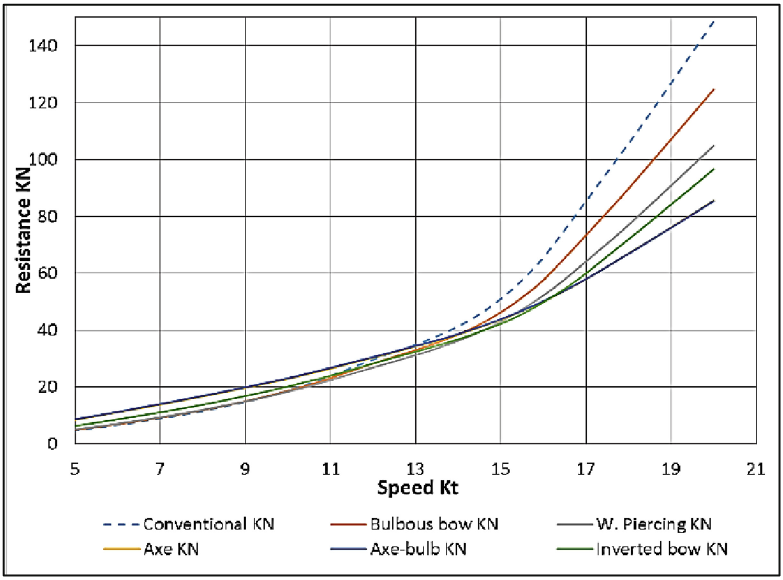

Fig. 9. Holtrop resistance prediction

Table 7. Holtrop resistance prediction at 19 knots

Model	Resistance KN	Resistance reduction
1. Conventional	126.9	–
2. Bulbous bow	107.1	16%
3. Wave piercing	90.8	28%
4. Axe-standard	76.1	40%
5. Axe-bulb	76	40%
6. Inverted bow	84.2	34%

Table 8. Slender body resistance prediction at 19 knots

Model	Resistance KN	Resistance reduction
1. Conventional	125.3	–
2. Bulbous bow	120.1	4%
3. Wave piercing	118.2	6%
4. Axe-standard	96.2	23%
5. Axe-bulb	95.3	24%
6. Inverted bow	103.5	17%

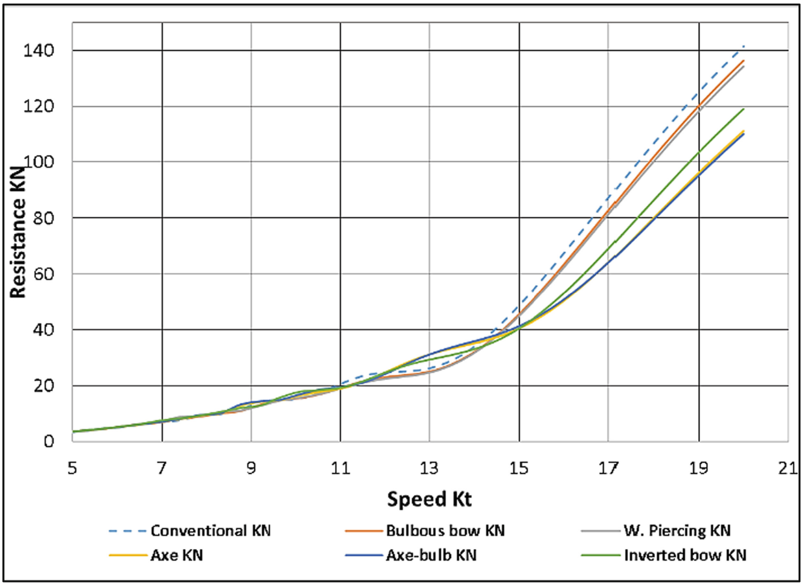

Fig. 10. Slender body theory resistance prediction

Figure 10 and Table 8 show each ship's resistance prediction using the slender body theory method. The Maxsurf Resistance software producer Bentley Systems (2013), uses a Michell paper (1898) based approach to compute the wave resistance of a port/starboard symmetrical mono hull to calculate the total resistance.

7 Hydrostatics

As the hull shape has been modified for each model, the hydrostatic conditions have changed especially the buoyancy longitudinal center (from Aft Perp.) and the water line length; the displacement was considered 294 ton and the trim of 0°. The results are shown in Table 9.

Table 9. Hydrostatic parameters for 294 ton displacement

Model	Buoyancy length	Waterline length	Draft
	m	M	m
1. Conventional	−2.08	43.90	1.845
2. Bulbous bow	−1.61	43.92	1.832
3. Wave piercing	−1.54	45.91	1.830
4. Axe-standard	1.06	52.74	1.682
5. Axe-bulb	1.17	52.74	1.681
6. Inverted bow	−0.07	48.33	1.739

8 Preliminary Seaworthiness

Seaworthiness is an important parameter to be analyzed due to that greater sea added resistance and accelerations decrease ship performance, comfort, and safety at sea. A number of previous studies (Ghassemi et al. (2015); Keuning and Pinkster (1995); Salvesen (1978); Faltinsen (1990) have investigated seakeeping behavior. The Maxsurf Motions software is a preliminary seakeeping analysis program using a linear strip theory method that is based on the work of Salvesen (1978). It is used to calculate in preliminary way the coupled heave and pitch response of the vessel and uncoupled roll motion.

8.1 Response Amplitude Operator Results

The Response Amplitude Operator (RAO), also referred to as a transfer function, describes how the response of a vessel varies with wave frequency. These RAOs are normally non-dimensional through the wave height or wave slope (Bentley Systems, Maxsurf Motions 2013). The RAO calculations in this paper were made using the Maxsurf Motions software using the linear strip theory method.

Waves at sea increase resistance due to ship motions. Figures 11 and 12 and Table 9 show the response amplitude operators (RAO), including added resistance from waves for the six models at sea state 5 (wave amplitude 3.26 m) at 19 knots and with head waves. Salvesen (1978) and Prpić-Oršić et al. (2008) present computation methods for added resistance from waves (Table 10).

Table 10. Added resistance

Model	Added resistance (KN/m^2)
1. Conventional	83
2. Bulbous bow	86
3. Wave piercing	82.5
4. Axe-standard	72
5. Axe-bulb	73
6. Inverted bow	84

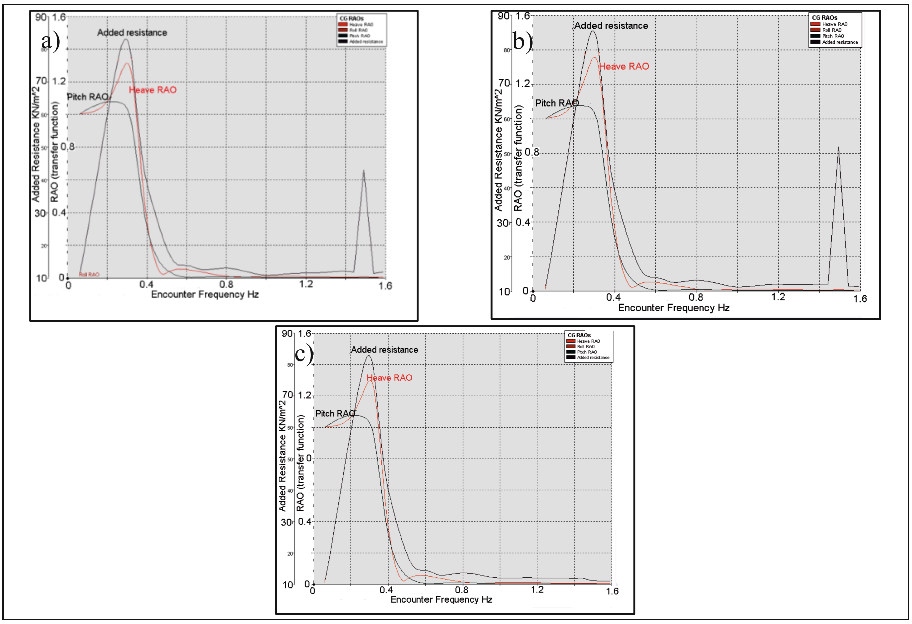

Fig. 11. RAO - head waves – (a) model 1 (b) model 2 (c) model 3

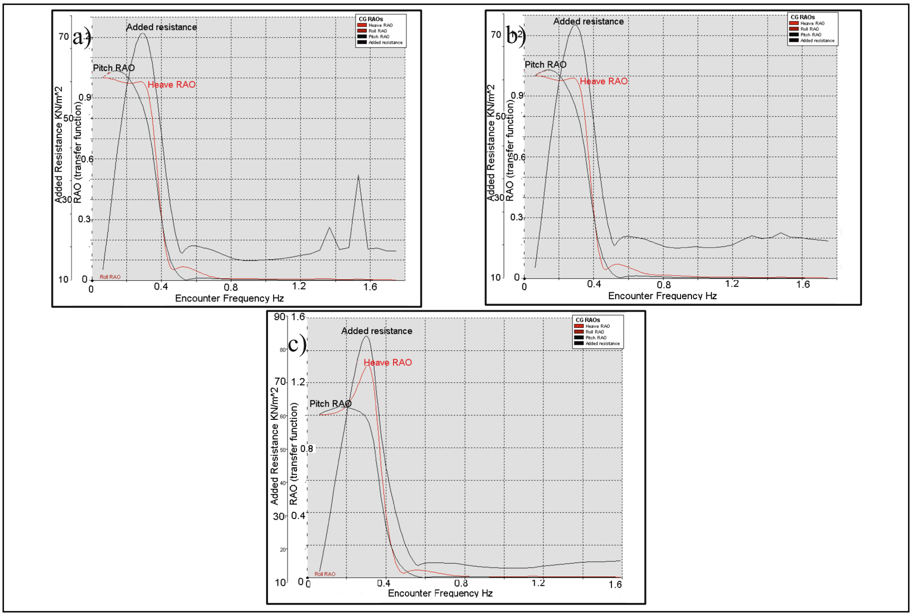

Fig. 12. RAO - head waves – (a) model 4 (b) model 5 (c) model 6

8.2 Motion Sickness Incidence Results

Motion Sickness Incidence (MSI) accelerations indicate the comfort of passengers, and the results obtained from Maxsurf Motions software are shown in Figs. 13 and 14, whereby the limits are according to ISO 2631/3 1985 recommendations. According to the Maxsurf Motions software, the calculation of the MSI is developed according to the McCauley et al. (1976) formulation, which includes an exposure time, while MSI accelerations are integrated over 1/3 octave bins and plotted against acceleration limits. The following equation is used:

$$MSI(\omega_{ecentre}) = \int_{\omega_{e1}}^{\omega_{e2}} S_{vertaccel}(\omega_e) d\omega_e$$

Where the frequency interval ωe1 to ωe2 is the 1/3 octave range centered about the ωe center and Svert accel is the absolute vertical acceleration. Bentley Systems (2013).

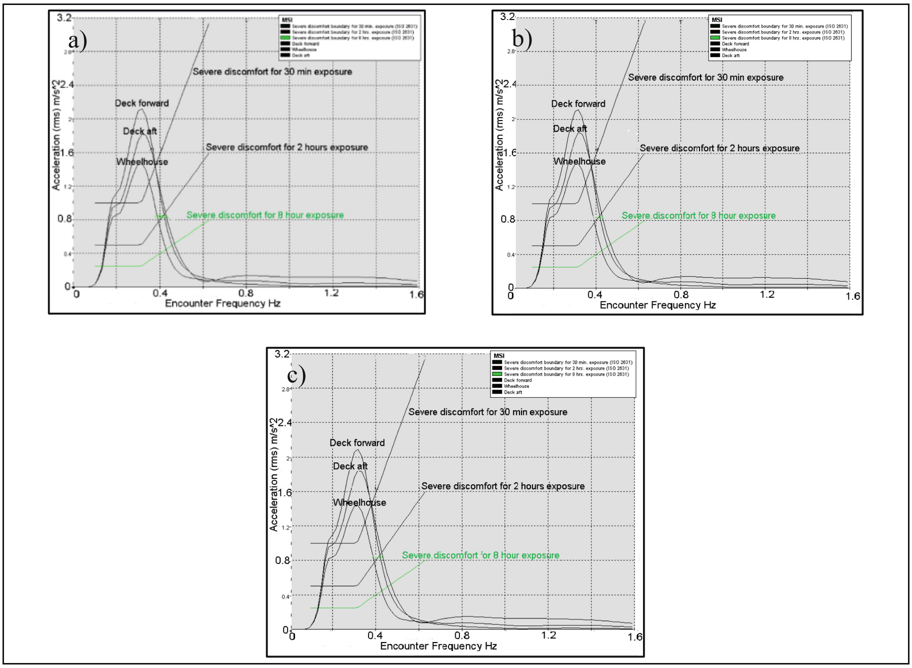

Fig. 13. MSI head waves – (a) model 1 (b) model 2 (c) model 3

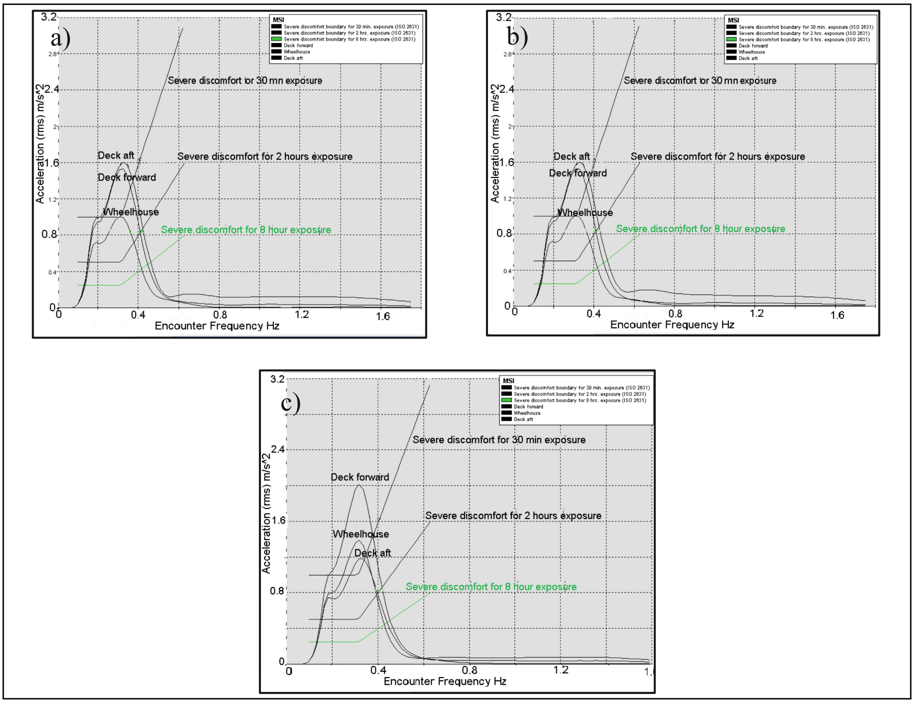

Fig. 14. MSI head waves – (a) model 4 (b) model 5 (c) model 6

9 Results and Discussion

The analyses conducted in this study offer the following results.

- The CFD results (resistance, heave and pitch) are close to the tank test results, as shown in Table 4, for a conventional hull at 19 knots. The difference between calculations was 0.3%, demonstrating the validity of the software for this calculation.
- The modified axe bow model (Model 5) shows better resistance reduction (35%) compared with the conventional models. This model result the better option because improves ship efficiency due to its fine and slender bow, while an improved reduction in MSI acceleration is also demonstrated upgrading ship comfort.
- Regarding wave added resistance, the modified axe bow model (Model 5) shows the smallest added resistance improving performance and decreasing fuel consumption at sea.
- The inverted bow model (Model 6) shows considerable resistance reduction (23%) and a slight comfort upgrade compared to the conventional model (Model 1).
- As can be seen in the figures showing the free surface elevation and dynamic pressure, the modified axe bow (Model 5) shows less wave elevation and less dynamic pressure compared to the other models, thus avoiding loss of energy.
- The resistance reduction shown on the bulbous bow model (Model 2) and wave piercing model (Model 3), are 4% and 10%, respectively. These resistance reduction results are less than the other models studied.

10 Conclusions

This study shows the good accuracy for resistance prediction with the ORCA-3D CFD software, demonstrating that it can be used in the development of efficient hull forms.

According to the results, the modified axe bow model (Model 5) showed the best performance of the bow shapes analyzed in this work; its finer hull form allows a smooth water entrance, reducing dynamic pressures and increasing waterline length. This resistance reduction will enable a considerable fuel consumption reduction, thus reducing CO2 emissions.

It is recommended that further analysis should examine aft shape modification possibilities to increase ship performance and seaworthiness.

Acknowledgements. Special thanks are extended to ORCA 3D MARINE CFD AND SIMERICS for permission to use the CFD software results in this analysis. Special thanks also to ESPOL for permission to use the University licenses to conduct this study according to the investigation programs.

References

Bentley Systems: Maxsurf motions user manual, version 20 (2013)

Bentley Systems: Maxsurf resistance user manual, version 20 (2013)

Faltinsen, O.M.: Sea Loads on Ships and Offshore Structures. Cambridge University Press, Cambridge (1990)

Ghassemi, H., Majdfar, S., Gill, V.: Calculations of the heave and pitch RAO's for three different ship's hull forms. J. Ocean Mech. Aerospace Sci. Eng. **22** (2015)

Hirota, K.: Development of bow shape to reduce the added resistance due to waves and verification on full scale measurement. In: International Conference on Marine Research and Transportation, The Island of ISCHIA, Italy (2005)

Holtrop, J., Mennen, G.G.J.: An approximate power prediction method. Int. Shipbuilding Progress **29**, 166–170 (1982)

Holtrop, J.: A statistical re-analysis of resistance and propulsion data. Int. Shipbuilding Progress **31**, 363 (1984)

Keuning, J.A., Pinkster, J.: Optimization of the seakeeping behavior of a fast monohull. In: Fast 1995 Conference (1995)

Keuning, J.A., Pinkster, J., van Walree, F.: Further investigation into the hydrodynamic performance of the AXE bow concept. In: Proceedings of the 6th Symposium on High Speed Marine Vehicles, Castello di Baia, Italy, pp. II 25–II 38 (2002)

Kyriazis, G.: Bulbous bow design optimization for fast ships. M.Sc. thesis, Massachusetts Institute of Technology (1996)

Michell, J.H.: The wave resistance of a ship. Philos. Mag. **5**(45), 106–123 (1898)

McCauley, M.E., Royal, J.W., Wylie, C.D., O'Hanlon, J.F., Mackie, R.R.: Motion sickness incidence: exploratory studies of habituation, pitch and roll and the refinement of a mathematical model. Human Factors Research Inc., Technical Report 1733-2, 1976. (USN ONR contract N00014-73-C-0040)

Prpić-Oršić, J., Nabergoj, R., Trincas, G.: The methods of added resistance estimation for ships in a seaway. Pula, Croatia, Symposium Sorta (2008)

Salvesen, N.: Added resistance of ships in waves. J. Hydronaut. **12**(1), 24–34 (1978)

Takahei, T.: A study on the waveless bow Part I. J. Soc. N. A. Japan **108**, 53–61 (1960)

Takahei, T.: A study on the waveless bow Part II. J. Soc. N. A. Japan **109**, 73–85 (1961)

Wigley, W.C.S.: The Theory of the Bulbous Bow and Its Practical Application. Newcastle (1936)